Published in final edited form as:
Pharmacogenet Genomics. 2012 April ; 22(4): 273–284. doi:10.1097/FPC.0b013e328350e270.

The G671V variant of MRP1/ABCC1 links doxorubicin-induced acute cardiac toxicity to disposition of the glutathione conjugate of 4-hydroxy-2-*trans*-nonenal

Paiboon Jungsuwadee[a,c], **Tianyong Zhao**[a], **Elzbieta I. Stolarczyk**[a], **Christian M. Paumi**[a], **D. Allan Butterfield**[b], **Daret K. St.Clair**[a], and **Mary Vore**[a]

[a]Graduate Center for Toxicology University of Kentucky Lexington KY

[b]Department of Chemistry and Center of Membrane Sciences University of Kentucky, Lexington KY

[c]Department of Basic Pharmaceutical Sciences, School of Pharmacy, Husson University, Bangor, ME

Abstract

Doxorubicin (DOX)-induced acute cardiotoxicity is associated with the Gly671Val (G671V; rs45511401) variant of multidrug resistance-associated protein 1 (MRP1) (Circulation 2005; 112:3754). Redox cycling of DOX causes lipid peroxidation and generation of the reactive electrophile 4-hydroxy-2-*trans*-nonenal (HNE). Glutathione (GSH) forms conjugates with HNE, yielding GS-HNE, an MRP1 substrate; GS-HNE accumulation can also cause cellular toxicity. We investigated the sensitivity of a cell line expressing G671V to DOX, and its transport capacity towards GS-HNE, and established stable HEK293 cell lines over-expressing wild-type MRP1 (HEK_{MRP1}), G671V (HEK_{G671V}), and R433S (HEK_{R433S}), an MRP1 variant not associated with DOX-induced cardiotoxicity. In ATP-dependent transport studies using cell line-derived plasma membrane vesicles, the V_{max} (pmol/min/mg) for GS-HNE transport was lowest for G671V (69±4) and highest for R433S (972±213) compared to wild-type MRP1 (416±22), while K_m values were 2.8±0.4, ≥6.0 and 1.7±0.2 μM, respectively. In cells, the DOX IC_{50} (48 h) was not different in HEK_{MRP1} (463 nM) vs. HEK_{R433S} (645 nM), but this parameter was significantly lower in HEK_{G671V} (181 nM). HEK_{G671V} retained significantly (~20%) more, while HEK_{R433S} retained significantly less intracellular DOX than HEK_{MRP1}. Similarly, HEK_{G671V} cells treated with 1.5 μM DOX for 24 h retained significantly more GS-HNE. In cells treated with 0.5 μM DOX for 48 h, GSH and GSSG levels and the GSH/GSSG ratio were significantly decreased in HEK_{G671V} vs. HEK_{MRP1}; these values were similar in HEK_{R433S} vs. HEK_{MRP1}. These data suggest that decreased MRP1-dependent GS-HNE efflux contributes to increased DOX toxicity in HEK_{G671V} and potentially in individuals carrying the G671V variant.

Keywords

ABCC1; doxorubicin; single nucleotide polymorphisms; cardiotoxicity

Corresponding author: Dr. Mary Vore, Graduate Center for Toxicology, University of Kentucky, 1095 V.A. Drive, 306 HSRB Lexington, KY 40536, Tel: 859-257-3760, Fax: 859-323-1059, maryv@uky.edu.

Introduction

Cardiac toxicity is one of the most serious and well known adverse reactions related to the administration of doxorubicin (DOX) and is dose-dependent. DOX is one of the active components in a current standard treatment regimen for breast cancer. In 2004, approximately 189,000 women and men were diagnosed with breast cancer, according to the Centers for Disease Control and Prevention. On average, cardiac toxicity occurs in 5% of these cancer patients [1], translating into more than 9,000 cardiac toxicity cases and an annual death rate of almost 2,000 patients in the US alone. While DOX cardiac toxicity is minimized by adherence to a maximum recommended dose of <400 mg/m^2, it is noteworthy that cardiac toxicity is nevertheless observed in some populations receiving less than the maximum recommended dose [2], suggesting genetic involvement of an unpredictable and idiosyncratic adverse drug reaction. On the other hand, Allen [3] reported that DOX is well tolerated in some patients receiving doses over twice that of the recommended total dose, stressing the significance of individual differences [4]. Thus, genetic or environmental factors that can influence drug concentrations may explain individual variation in both efficacy and safety. The cardiac toxicity of DOX may be attributable in part to genetic variations in drug targets and/or genetic differences in drug disposition such as in biotransformation enzymes and drug transporters [5, 6].

Using polymerase chain reaction-single-strand conformation polymorphism analysis, Conrad et al [7] identified several multidrug resistance-associated protein 1 (MRP1/ABCC1) variants in 36 healthy Caucasian volunteers. Among several variants, they identified Arg433Ser (R433S), located in the second transmembrane spanning domain, and Gly671Val (G671V; rs45511401), near the Walker A motif in the first nucleotide binding domain. The R433S MRP1 variant showed a 50% decreased transport maximum for leukotriene C4 (LTC_4) [8], however, cells expressing this variant were more resistant to DOX than those expressing wild-type MRP1 [8]. The G671V variant showed no difference in *in vitro* transport assays using LTC_4 or estradiol-17β-glucuronide ($E_2$17G) as substrates. Wang et al [9] sequenced 142 individuals of 4 different populations (Chinese, Malay, Indian and Caucasian) and found the frequencies of both of these SNPs to be less than 3%. The frequency of the G671V variant (Exon 16, 2012G>T) was 2.78% for the T allele in Caucasians, and 1.43% in the Indian population, with none reported in the Asian population [9]. Wang et al [9] reported the functional effects of these non-synonymous SNPs predicted by using SIFT, PolyPhen and PANTHER to be potentially adverse. Importantly, in a nested case-control cohort clinical study, patients with the G671V variant showed a significantly increased DOX-induced acute cardiac toxicity that accounted for 6.4% of the incidence of acute cardiac toxicity, with an Odds Ratio (OR) of 3.6 (95% Confidence Interval 1.6 to 8.4) [10]. Whether this was due to an increased accumulation of intracellular DOX or a decreased capacity for effluxing other MRP1 substrates is not known.

Upon administration, the quinone moiety of DOX undergoes redox cycling and induces oxidative stress, which in turn initiates lipid peroxidation and production of highly reactive lipid aldehydes, such as 4-hydroxy-2-*trans*-nonenal (HNE). HNE is detectable in heart tissues as early as 3 h following DOX administration [11-14]. HNE is an α,β-unsaturated aldehyde derived from ω-6 polyunsaturated fatty acids, such as linoleic acid and arachidonic acid [15, 16], and is one of the primary and highly toxic products of lipid peroxidation. HNE is a potent electrophile with high reactivity towards cellular nucleophiles. Protein residues known to react with HNE are cysteine, histidine and lysine [15], leading to the hypothesis that these products of lipid peroxidation play a central role in initiating functional impairment of the myocardium following treatment with DOX. HNE also reacts with intracellular glutathione (GSH) to form glutathione-conjugated HNE (GS-HNE) [17, 18], which is less toxic than HNE, but still retains some toxicity [19, 20] so that its clearance is

warranted. Thus, metabolic removal of HNE could play an important role in protecting against myocardial injury.

While several mechanisms are involved in DOX-induced cardiac toxicity, oxidative damage appears to be the key component of such toxicity. In addition, based on the fact that 1) cumulative doses of DOX are a risk for DOX-induced cardiac toxicity, 2) HNE and HNE metabolites (e.g., GS-HNE) have been shown to be associated with oxidative stress in a myocardial ischemic model [21], and 3) MRP1 is highly expressed in heart [22, 23], we postulated that the association of the MRP1 G671V variant with DOX-induced acute cardiac toxicity [10] could be due to a change in its substrate specificity. In this study, we examined whether cells expressing the G671V and R433S variants vs. wild-type MRP1 were more sensitive to DOX, and characterized the transport properties of wild-type MRP1 relative to the G671V and R433S MRP1 variants, specifically with respect to GS-HNE transport activity.

Material and methods

Reagents

[^{3}H]LTC_4 (160 Ci/mmol) and [^{3}H]GSH ([glycine-2-^{3}H]; 41.5 Ci/mmol) were purchased from PerkinElmer Life Sciences (Boston, MA) and G418 from Gibco (Invitrogen, Carlsbad, CA). GSH and GSH ethyl ester (GEE) were purchased from Sigma Aldrich (St. Louise, MO), Hoescht 33342 and Alexa Fluor488 from Molecular Probes (Eugene, OR), DOX HCl from Bedford Laboratories (Bedford, OH), MRP1 monoclonal antibody (MRPr1) from Alexis (San Diego, CA), mouse anti-sodium/potassium-ATPase α-1 (Na^+/K^+-$ATPase_{α-1}$) mAb from Millipore (Temecula, CA) and donkey anti-rabbit Cy3 from Jackson Immuno Research Laboratories (West Grove, PA). Anti-rat Ig-, anti-rabbit Ig-, and anti-mouse Ig-HRP and ECL-Plus, were obtained from Amersham Biosciences (Piscataway, NJ).

Vector Construction and Site-directed Mutagenesis

The plasmid pCMV/MRP1 containing MRP1 cDNA was a generous gift from Dr. Piet Borst (Division of Molecular Biology, the Netherlands Cancer Institute, Amsterdam, Netherlands). For construction of an MRP1 expression vector containing a neomycin selectable marker, the MRP1 coding region was amplified by PCR using plasmid pCMV/MRP1 as template and using two gene specific primers (forward primer: 5′-GCGATATCATGGCGCTCCGGGGCTTCTGCAGCG-3 ′; reverse primer: 5 ′-TATGCGGCCGCTCACACCAAGCCGGCGTCTTTGGCC-3′). Two restriction enzyme sites, EcoRV and NotI, were included in the primers to facilitate cloning. The PCR products were purified with a PCR purification kit according to the manufacturer's instructions (Qiagen; Valencia, CA), digested with EcoRV and NotI, and purified on an agarose gel (Qiagen). The purified fragment was inserted into the corresponding sites of the plasmid pUSEamp(+) (Millipore), which contains a neomycin selectable marker. MRP1 variants of G671V and R433S were generated using the QuickChange® II XL site-directed mutagenesis kit (Stratagene, La Jolla, CA) according to the manufacturer's instructions with the following mutagenic primers (for G671V, forward primer TCCATCCCCGAAGTTGCTTTGGTGGCCGTG and reverse primer CACGGCCACCAAAGCAACTTCGGGGATGGA; for R433S, forward primer GTGGACGCTCAGAGCTTCATGGACTTGGC and reverse primer GCCAAGTCCATGAAGCTCTGAGCGTCCAC). MRP1 and MRP1 variants in expression constructs were sequenced in both forward and reverse directions to confirm the correct sequences (MWG, High Point, NC). HEK293 cells were transfected with expression vectors of wild-type MRP1, MRP1 variants, or empty vector using TransIT293 transfection reagent. Stable transfected cells were obtained after 10-14 days selection with G418 (600 μg/ml).

The stable transfected cells were tested for MRP1 expression by Western blot analysis or immunofluorescent staining. Cells were maintained in culture media containing G418 (300 μg/mL) until use.

Flow cytometry

In order to quantitate MRP1 expression in the transfected cell lines, cells were fixed with 2% paraformaldehyde for 10 min and then permeabilized in cold methanol for 20 min on ice. Cells were washed twice in FACS buffer (2% FBS in PBS) and stained with MRPr1 antibody (1:100) for 1 h at room temperature, washed twice and incubated with AlexaFluor 488-conjugated secondary antibody (1:500) for 1 h at room temperature and protected from light. Samples were subjected to analysis using a flow cytometer (BD-LSR model, Becton-Dickinson, San Jose, CA). Twenty thousand events of live cells were analyzed for each sample. The strength of the fluorescence was depicted in terms of mean fluorescence intensity (MFI). Flow cytometry studies were performed by the University of Kentucky Flow Cytometry Core Facility.

RNA Isolation and Real-Time RT-PCR Analysis of Gene Expression

Total RNA from transfected HEK293 cells was isolated by using the GenElute Mammalian Total RNA Miniprep Kit from Sigma-Aldrich (Milwaukee, WI). The cDNA was synthesized by using SuperScript® III Reverse Transcriptase from Invitrogen according to the manufacturer's instructions. Primers and UPL probes for real time RT-PCR were designed and ordered from Roche Applied Science (Mannheim, Germany) by using online software (http://www.universalprobelibrary.com), and real-time RT-PCR was determined with the use of a 480 LightCycler (Roche Applied Sciences). For detection of MRP1 mRNA, primers MRP1-F (TGTGGGAAAACACATCTTTGA) and MRP1-R (CTGTGCGTGACCAAGATCC) were used with UPL probe 89. For detection of 18S RNA, primers 18S-F (CGATTGGATGGTTTAGTGAGG) and 18S-R (AGTTCGACCGTCTTCTCAGC) were used with UPL probe 81. In detail, 2 μg of total RNA was used for cDNA synthesis, and then the synthesized cDNA was diluted to 100 μL. Diluted cDNA (5 μL) was used as template in a 20-μL reaction volume. The target gene expression was normalized by its 18S RNA gene expression.

Animals

FVB and Mrp1-disrupted FVB ($Mrp1^{-/-}$, Taconic Transgenics, Hudson, NY) mice were maintained in the Division of Laboratory Animal Resources facility and provided food and water *ad libitum*. All experiments were approved by and complied with the requirements of the Institutional Animal Care and Use Committee of the University of Kentucky. Mice were treated intraperitoneally (ip) with DOX, 20 mg/kg, and the heart removed 24 h later.

Isolation of plasma membranes

Hearts were homogenized in buffer containing 0.225 M mannitol, 0.075 M sucrose, 1 mM EGTA, and protease inhibitors (1 mM phenylmethylsulfonyl fluoride, 1 μg/mL leupeptin, 1 μg/mL aprotinin, 1 μg/mL pepstatin), centrifuged at 480*g* for 5 min, and the pellet used to isolate sarcolemma as described [24]. Plasma membranes from HEK293 cells stably transfected with MRP1 and its variants were similarly prepared as described [24].

Synthesis and purification of GS-HNE

The [^{3}H]GSH-conjugate of HNE ([^{3}H]GS-HNE) was synthesized by incubating a 10-fold molar excess of HNE with [^{3}H]GSH in 100 mM Tris, pH 7.2 containing 2 units of rat liver glutathione-S-transferase (GST) [20]. The reaction was performed at 37°C for 2 h or until the concentration of HNE remained stable, as monitored by the HNE absorbance at 224 nm.

Unlabeled GS-HNE was generated by incubation of freshly prepared GSH with HNE in a 4:1 molar ratio in the presence of 20 mM potassium phosphate buffer, pH 6.8 at 37°C with gentle mixing [20]. The reaction mixtures were purified by HPLC on a Symmetry C18, 4.6x250 mm column (Waters Corporation Milford, MA) by using a linear gradient from 0% to 100% solvent B [0.05% trifluoroacetic acid (TFA) in acetonitrile] in solvent A (0.05% TFA in water) over 25 min at a flow rate of 1 ml/min. The column effluent was monitored at 210 nm, and peak fractions (retention time between 11-13 min) were collected, lyophilized and redissolved in absolute ethanol. The concentration of GS-HNE was measured colorimetrically [20].

Immunoblot analysis

Whole cell lysate or plasma membrane protein samples were fractionated by SDS-PAGE, 4-12% polyacrylamide gel, transferred onto a nitrocellulose membrane and blocked with 5% nonfat dried milk in a Tris-buffered saline Tween-20 (TBS-T; 10 mM Tris-HCl, pH 7.8, 150 mM NaCl, and 0.1% Tween 20) buffer pH 7.8 for 1 h at room temperature. Membranes were incubated with the primary antibodies for MRP1 (1:1000) and Na^+/K^+-$ATPase_{\alpha 1}$ (1:20,000), washed three times, each for 5 min with TBS-T, followed by incubation with the secondary antibody (1:5000) 1 to 2 h at room temperature, and finally washed twice with TBS-T buffer for 5 min. Proteins were detected using the enhanced chemiluminescence detection system (ECL Plus®, Amersham Biosciences).

Fluorescent microscopy

HEK293 transfected cells were cultured to reach 80% confluence. Cell nuclei were stained with Hoescht 33342 and incubated at 37°C for 5 min. Cells were washed with PBS, fixed with 4% paraformaldehyde, permeabilized with 0.2% Triton X-100, blocked with 1% BSA in PBS, and incubated with primary antibody against MRP1 (1:2500) and probed with secondary antibodies (AlexaFluor 488 1:1000 in 1% BSA in PBS) as described [24]. Cells were washed, rinsed with ddH_2O, air-dried, mounting medium added and the cells placed under a cover glass [24]. Images were taken using an Olympus IX71 fluorescent microscope.

Transport assays

The transport experiments were performed as described [24]. Sarcolemma or plasma membrane vesicles were made by vesiculation through a 25G needle 15 times before the transport assay. ATP-dependent transport of [^{3}H]GS-HNE into plasma membrane vesicles (5 μg protein/20 μL) was measured in incubations at 37°C for 1 min, while that of [^{3}H]LTC_4 was measured at 23°C for 1 min [24, 25]. Reactions were terminated, filtered and radioactivity sequestered within the inside-out vesicles detected as described [24].

Cytotoxicity and DOX retention assays

To determine cytotoxicity, cells ($2.5x10^4$/well) were seeded onto a 96-well plate and cultured in the presence of DOX at various concentrations. After 45 h, 20 μL of Methylthiazol tetrazolium (MTT, 5 mg/mL) was added to each well and cultures continued for an additional 3 h. Supernatants were discarded, 100 μL DMSO added to dissolve the formazan crystal and its concentration determined by spectrophotometry at A_{540}. The MTT values (absorption expressed as a percentage of control values) obtained after continuous 48 h exposure of cells to DOX were compared, and the DOX concentrations inhibiting cell growth by 50% (IC_{50}) calculated from the per cent survival curves.

To determine cellular retention of DOX, cells ($5x10^5$/well) were plated and cultured in 24-well plates using 6 wells per cell line. After 24 h in culture, cells were treated with 50 μM

DOX for 1 h, the media replaced with fresh media, and cells incubated for an additional 30 min in the absence of DOX. Cells were washed twice with PBS, 800 μL of buffer (50 mM Tris-HCl, pH 8.0, 150 mM NaCl, 1% NP-40, 0.5% deoxycholate and 0.1% SDS) added to each well to lyse cells, and 200 μL of cell lysate assayed for DOX by fluorescence spectroscopy (excitation at 460/40; emission at 560/15 nm). In a separate experiment in which the 30 min efflux step was omitted, cells ($2.5x10^5$/well) were plated and cultured for 24 h, treated with 1.5 μM DOX and cultured for an additional 24 h. DOX retained in cells was assessed as above, and retained GS-HNE assessed as described below.

HPLC Assay of GSH, GSSG and GS-HNE

Cells were treated with DOX (0.5 or 1.5 μM) for 0, 4, 24 or 48 h as indicated in figure legends, and GSH, GSSG and GS-HNE quantitated by HPLC. Cells were washed once with PBS and harvested by trypsinization. Pellets were washed three times in cold PBS, resuspended in cell lysis buffer (1% Triton X-100, 0.2 M NaCl, 0.1 M Tris-HCl with Complete mini® protease inhibitor), incubated on ice for 20 min and centrifuged at 4000*g* at 4°C for 5 min. For GS-HNE analysis, supernatants were subjected directly to HPLC analysis using the same conditions described for the synthesis and purification of GS-HNE. For GSH and GSSG quantitation, whole cell lysates were used for GSH derivatization as described [26] with minor modifications. Five percent trichloroacetic acid, 7.5 mM *N*-ethylmaleimide, and 100 mM dithiotheitol were prepared in redox quenching buffer (20 mM HCl, 5 mM diethylenetriaminepentaacetic acid, 10 mM ascorbic acid) [26]. Monobromobimane (50 mM) was dissolved in HPLC-grade acetonitrile-Triethanolamine (1 M, pH 8.2). The derivatized samples were centrifuged and the supernatant assayed for thiol-bimane fluorescence by reverse-phase HPLC using a linear gradient from 0% to 100% solvent B (50% Methanol, 0.25% acetic acid in water) in solvent A (10% Methanol, 0.25% acetic acid in water) over 28 min at a flow rate of 0.8 mL/min with fluorescence detection at Ex_{370}/Em_{485} using the Waters 2475 Multi λ fluorescence detector as described [26]. Fluorescence intensities versus time of elution were quantitated using Waters Breeze chromatography software v. 3.2 and peak areas integrated and converted to nmol GSH equivalents from the integrated areas under the GSH standard curve.

Statistical Analysis

Data of quantitative results were expressed as mean ± SEM, or as otherwise indicated. Statistical analyses were performed using one-way ANOVA followed by a post-hoc test using GraphPad Prism 4. A p value <0.05 was considered as a significant difference. IC_{50} values were obtained by nonlinear regression analysis to obtain the best-fit values and the 95% Confidence Interval of these values, as determined by GraphPad Prism 4. The kinetic parameters, K_m and V_{max}, and their 95% Confidence Interval were determined by fitting all of the data to the Michaelis-Menten equation, as determined by GraphPad Prism 4.

Results

HEK_{G671V} cells are more sensitive to DOX cytotoxicity than HEK_{MRP1} and HEK_{R433S}

Patients with the G671V variant showed a significantly increased DOX-induced acute cardiac toxicity [10]. In an attempt to understand this phenomenon, we developed HEK293 cell lines that stably expressed human MRP1 single nucleotide polymorphisms (SNPs) G671V, and three different control cells: HEK293 cells transfected with pUSE(amp)+ vector (HEK_{pUSE}), wild-type (WT) MRP1 (HEK_{MRP1}), or the R433S variant (HEK_{R433S}), which is not associated with DOX-induced acute cardiac toxicity. To confirm MRP1 expression and localization, we immunostained the cells for MRP1 as shown in Fig. 1; while HEK_{pUSE} did not express MRP1, the wild-type and MRP1 variants showed high MRP1 protein expression in the plasma membrane (Fig 1a). Expression levels of MRP1 did not differ among the

MRP1-transfected cells lines with respect to either protein or mRNA level, as measured by flow cytometry (Fig. 1b) and RT-PCR (Fig. 1c), respectively.

To determine the impact of the G671V SNP on cell viability and estimate the DOX IC_{50} value, we cultured cells in the presence of DOX at various concentrations for 48 h (Fig. 2a); IC_{50} values were calculated from the per cent survival curves (Fig. 2b). As shown in Fig. 2a, HEK_{G671V} cells were more sensitive to DOX than HEK_{MRP1} cells, while HEK_{R433S} cells were not significantly different from HEK_{MRP1} cells (Fig. 2b). All three MRP1 overexpressing cells were more resistant to DOX than HEK_{pUSE} control cells.

HEK_{G671V} cells retain more DOX and GS-HNE than HEK_{MRP1} and HEK_{R433S} cells

Cytotoxicity of DOX is dependent upon its intracellular cumulative concentration, and is decreased via MRP1-dependent efflux. To determine whether the G671V variant influenced retention of DOX, we incubated cells with DOX (50 μM, 1 h) and then cultured cells for an additional 30 min in the absence of DOX to determine its MRP1-mediated efflux. We also incubated cells with 1.5 μM DOX for 24 h and then measured intracellular DOX to determine DOX retention at steady state. Following a 1 h-incubation, HEK_{G671V} cells retained 20% more DOX, while HEK_{R433S} cells retained significantly less DOX compared to HEK_{MRP1} cells (Fig. 3a). There was no difference in DOX retention following the 24-h incubation between HEK_{G671V} and HEK_{MRP1} (Fig 3b). As expected, the highest DOX accumulation occurred in HEK_{pUSE} cells. Interestingly, DOX retention in HEK_{R433S} was less than that in HEK_{MRP1} cells following both 1 and 24 h of incubation (Fig. 3a and 3b).

DOX initiates reactive oxygen species and causes lipid peroxidation, with HNE as one of the major toxic lipid metabolites. The highly electrophilic HNE reacts rapidly with nucleophiles, particularly GSH, to form GS-HNE. Despite its decreased reactivity, GS-HNE remains toxic and requires an efflux transporter to eliminate it from cells [20]. We therefore characterized the retention of GS-HNE in HEK_{pUSE}, HEK_{MRP1}, HEK_{G671V} and HEK_{R433S} cells following treatment with 1.5 μM DOX for 24 h. As shown in Fig. 3c, treatment with DOX significantly increased GS-HNE in both HEK_{pUSE} and HEK_{G671V} cells, and GS-HNE retention was significantly greater in HEK_{G671V} than in HEK_{MRP1} or HEK_{R433S} cells (Fig. 3d).

HEK_{G671V} cells have decreased GSH/GSSH ratios compared to HEK_{MRP1} cells

GSH is an important antioxidant in protecting cells from oxidative damage so that a decrease in the GSH/GSSG ratio provides a measure of the degree of oxidative stress in cells, which is associated with cardiovascular diseases [27]. To determine whether the decreased DOX IC_{50} in HEK_{G671V} was due to more severe oxidative stress, we measured intracellular GSH and GSSG and calculated the GSH/GSSG ratios in cells cultured in media alone or in the presence of DOX (0.5 μM) for 4, 24 and 48 h. GSH and GSSG were highest in HEK_{pUSE} and lowest in HEK_{G671V} at all time points after DOX treatment, while GSH and GSSG were similar in HEK_{MRP1} and HEK_{R433S} cells at all time points (Fig. 4a and 4b). The GSH/GSSG ratio in HEK_{MRP1} was well-maintained throughout DOX exposure, but was higher in HEK_{R433S} up to 24 h (Fig. 4c, insert). Consistent with their decreased DOX IC_{50}, the GSH/GSSG ratio in HEK_{G671V} was lower than all other cell lines at all time points of DOX exposure (Fig. 4c), and was significantly decreased at 48 h after DOX (Fig. 4c, insert).

To determine whether augmenting intracellular GSH might increase cell survival in HEK_{G671V} cells treated with DOX, we supplemented these cells with GSH or GEE, a GSH prodrug. Supplementation of the culture media with GEE for 48 h significantly increased intracellular GSH levels in HEK_{G671V} in a dose-dependent manner (Fig. 5a), but did not increase cell survival following treatment with DOX (0.5 μM, 48 h) (Fig. 5b). However,

inhibition of MRP1 with MK571 further reduced the percent survival of HEK_{G671V}, regardless of supplementation of the media with GSH or GEE (Fig. 5b). These data further supported the importance of MRP1 transport activity in protecting cells against DOX-induced toxicity.

G671V SNP maintains LTC_4 transport activity but loses GS-HNE transport capacity

In view of the cellular GS-HNE retention in HEK_{G671V} cells, we examined further whether the MRP1 polymorphisms would have an impact on their substrate specificity or transport capacity. We first characterized transport of the classic MRP1 substrate, LTC_4, in plasma membrane vesicles after normalization for expression of MRP1 (Fig. 6a). The G671V variant was comparable to wild-type MRP1 with respect to LTC_4 transport, while LTC_4 transport was decreased by 75% in the R433S variant compared to wild-type MRP1 (Fig. 6b), consistent with previous reports [7, 8]. To determine if the G671V variant might have an altered dependence on GSH for transport, we examined the effects of GSH; 0.5 mM GSH had no effect on transport, while 5 mM GSH completely inhibited LTC_4 transport by MRP1 and both its variants (Fig. 6b).

We next determined the kinetic parameters for GS-HNE transport in plasma membrane vesicles. GS-HNE was transported via Michaelis-Menten kinetics (Fig. 6c), and showed a markedly reduced transport by the G671V variant such that the V_{max} was decreased to about 15% of that by wild-type MRP1 (Fig. 6c). In contrast, the V_{max} of the R433S variant was increased over 2-fold relative to wild-type MRP1. The K_m value of the G671V variants did not differ significantly from that of wild-type MRP1 (Fig. 6c), and agreed well with the K_m of 1.6 μM reported previously for MRP1 [20]. The estimate of the K_m for the R433S variant was higher (≥6 μM), consistent with its increased V_{max} (Fig 6c). The V_{max}/K_m of the G671V variant was only about 10% (0.025 mg/l/min) of that of wild-type MRP1 (0.24 mg/l/min), indicating a markedly decreased transport efficiency of the G671V variant.

Mrp1 is a major transporter for GS-HNE in mouse heart

The loss of MRP1-mediated GS-HNE transport could be significant if this transporter were the main mechanism for the heart to eliminate GS-HNE. To investigate whether the cardiac sarcolemma can transport GS-HNE, and the importance of Mrp1, we isolated sarcolemma membranes from FVB wild-type and $Mrp1^{-/-}$ mice that were treated with DOX (20 mg/kg, i.p.) and killed 24 h later. As shown in Fig. 7, sarcolemma from FVB mice transported GS-HNE in a saturable manner, with a K_m and V_{max} of 2.5 ± 1.1 μM and 911 ± 166 pmol/min/mg protein, respectively. Transport of GS-HNE was not detectable in sarcolemma vesicles prepared from $Mrp1^{-/-}$ mice (Fig. 7), indicating that Mrp1 was the sole transporter mediating GS-HNE transport.

Discussion

The increased incidence of acute DOX-induced cardiac toxicity in patients who carry the G671V variant of MRP1 suggests that the glycine to valine variant at amino acid 671 of MRP1 affects its transport function for certain substrates. Consistent with this hypothesis is the result predicted by PolyPhen-2 (http://genetics.bwh.harvard.edu/pph2/) in which this G671V variant is predicted to be “probably damaging”, likely due to the proximity of G671 to the Walker A motif. The present studies provided clear evidence that the ability to transport GS-HNE was profoundly decreased by 85% in the G671V MRP1 variant relative to wild-type MRP1. In a previous study [7], the G671V variant did not show altered transport of several MRP1 substrates (LTC_4, estrone sulfate and $E_2$17G), and in this study we confirmed that transport of LTC_4 was not impacted. These data further support our understanding of the differential effects of changes in amino acid sequence on transport

characteristics of various substrates for MRP1, and other MRP transporters [28-30]. Characterization of the DOX IC_{50} values revealed that amongst MRP1 expressing cell lines, HEK_{G671V} cells were the most sensitive to its cytotoxic effects (Fig. 2). HEK_{G671V} retained about 20% more DOX than did HEK_{MRP1} and HEK_{R433S} (Fig. 3a), and this could contribute to the decreased DOX IC_{50} from 463 nM in HEK_{MRP1} to 181 nM in HEK_{G671V}. In contrast, HEK_{R433S} cells retained less DOX than HEK_{MRP1} cells, but these two cell lines did not differ in their IC_{50} values. These data are in contrast to an earlier report [8] showing that HeLa cells expressing R433S are 2-fold more resistant than cells expressing wild-type MRP1. The bases for the different findings are not known, but likely reflect the use of different cell lines. As expected, HEK_{pUSE} cells retained the greatest amount of DOX, and were the most sensitive to DOX-induced cytotoxicity.

We next examined cellular GS-HNE levels after treatment of cells with 1.5 μM DOX for 24 h and found that HEK_{G671V} cells retained the highest amount of this MRP1 substrate. We also measured the redox status of GSH and GSSG in each of the cell lines in response to DOX treatment. GSH and GSSG were highest in HEK_{pUSE} cells, consistent with the known GSH- and GSSG-efflux activities of MRP1. GSH and GSSG levels decreased across time following DOX exposure in all cell lines, and were lowest at all time points in HEK_{G671V} cells. The loss of GSH exceeded that of GSSG, so that the GSH/GSSG ratio was also lowest at all time points in HEK_{G671V} cells, indicating that these cells were under the most oxidative stress. In view of the lack of effect of GSH supplementation on the viability of HEK_{G671V} cells in the presence of DOX, and their further decreased survival in the presence of the MRP1 inhibitor MK571, we characterized the GS-HNE transport capacity of the wild-type and variant forms of MRP1. Based on V_{max} values, the GS-HNE transport capacity of the G671V variant was decreased 85% relative to wild-type MRP1 (Fig. 6c), and exhibited a 10-fold decrease in V_{max}/K_m. These data imply that GS-HNE accumulated in HEK_{G671V} cells due to the loss of MRP1 efflux activity. It is important to note that GS-HNE remains toxic to cells [20], most likely because it mediates feed-back inhibition of glutathione-S-transferases that catalyze the conjugation of GSH and HNE, resulting in accumulation of HNE and an attendant cytotoxicity [31]. Alternatively, but with lesser likelihood, Schiff base formation between GS-HNE and Lys residues on proteins could also play a role in its toxicity [15, 16].

These data are consistent with the decreased survival of HEK_{G671V} cells in the presence of MK571, a classic MRP inhibitor, despite increased intracellular concentrations of GSH induced by incubation with GEE (Fig. 5a). The present data also indicate the importance of MRP1 in effluxing GS-HNE from the heart, since sarcolemma membrane vesicles from mice deficient in Mrp1 showed no GS-HNE transport activity (Fig. 7). These data are consistent with the early identification of an efflux mechanism in the heart for GS-HNE [32]. These are the first data demonstrating that the G671V variant has a decreased capacity to efflux GS-HNE, despite retention of the ability of this MRP1 variant to transport other classic MRP1 substrates, i.e., LTC_4, estrone sulfate, and E_217G [7]. It is also interesting to note that the R433S variant showed significantly increased transport of GS-HNE, despite decreased transport of LTC_4 (Fig. 6b) and estrone sulfate, and unaltered transport of E_217G [8]. Systematic mutation of amino acid residues in MRP1 has provided numerous examples demonstrating selective alteration of transport of substrates [33, 34]. In a study comparing the substrate specificities of MRP1 and MRP3, Grant et al [30] substituted amino acids 425-516 of MRP1 in the region spanning transmembrane helices 8 and 9 with those of amino acids 411-502 of MRP3, and found complete loss of LTC_4 transport, but a modest enhancement of $E_217\beta G$ transport, with minimal effects on transport of methotrexate, a substrate common to both MRP1 and MRP3 [30]. A cluster of 3 amino acids (Tyr440, Ile441 and Met443) in MRP1 and Phe426, Leu427 and Leu429 of MRP3 made major contributions to these differences. The conclusion of these authors that amino acids in this

region of MRP1/MRP3 make significant contributions to substrate specificity is consistent with the current findings that the Arg433 of MRP1 also selectively influenced MRP1 substrate specificity. Interestingly, alignment of this region of MRP1 ([29]; Figure 2) shows that Arg433 of MRP1 is conserved in MRP3, MRP5, MRP6 and MRP7, and is replaced with a lysine in MRP2 and MRP4, suggesting the importance of a cationic amino acid in this position.

Gly671 is 7 amino acids upstream of the Walker A motif of NBD1 in MRP1, and is conserved in CFTR, TAP1, YCF1 and some bacterial ABC transporters [33], again implying an important function. Despite its location close to the Walker A motif, the substitution of a valine must not have affected the rate of ATP hydrolysis, based on the retention of LTC_4 transport.

In conclusion, cells expressing the G671V MRP1 variant were more sensitive to DOX than cells expressing wild-type MRP1, most likely due to an increase in accumulation of intracellular GS-HNE, together with a decrease in the GSH/GSSG ratio, indicating oxidative stress that can lead to cytotoxicity. While increased retention of DOX could also contribute to the increased oxidative stress in cells expressing the G671V variant, because amino acids in the third membrane spanning domain, especially between amino acids 959 and 1187, are considered most critical for DOX transport [35], it seems less likely that the G671V variant alters MRP1 recognition of DOX. The decreased GS-HNE transport capacity of the G671V variant further indicates that MRP1 polymorphisms can play a significant role in MRP1 activity, and that these findings may be clinically important in patients receiving chemotherapy, particularly DOX. Close monitoring for cardiac toxicity may therefore be beneficial in patients with the MRP1 G761V polymorphism who are receiving DOX chemotherapy.

Acknowledgments

This study was supported by National Institutes of Health grant CA139844 and CTSA UL1RR033173.

Abbreviations list

DOX	Doxorubicin
DMSO	Dimethylsulfoxide
DTT	Dithiothreitol
GEE	glutathione ethyl ester
GSH	Glutathione
GSSG	Glutathione disulfide
HNE	4-hydroxy-2-*trans*-nonenal
HRP	Horseradish peroxidase
K_m	Michaelis constant
MRP1	Multidrug resistance-associated protein 1
NEM	*N*-ethylmaleimide
TBS	Tris-buffered saline
TEA	Triethanolamine
V_{max}	Maximum velocity

References

1. Shan K, Lincoff AM, Young JB. Anthracycline-induced cardiotoxicity. Ann Intern Med. 1996; 125:47–58. [PubMed: 8644988]
2. Henderson IC, Allegra JC, Woodcock T, Wolff S, Bryan S, Cartwright K, et al. Randomized clinical trial comparing mitoxantrone with doxorubicin in previously treated patients with metastatic breast cancer. J Clin Oncol. 1989; 7:560–571. [PubMed: 2468745]
3. Allen A. The cardiotoxicity of chemotherapeutic drugs. Semin Oncol. 1992; 19:529–542. [PubMed: 1411651]
4. Wojtacki J, Lewicka-Nowak E, Lesniewski-Kmak K. Anthracycline-induced cardiotoxicity: clinical course, risk factors, pathogenesis, detection and prevention--review of the literature. Med Sci Monit. 2000; 6:411–420. [PubMed: 11208348]
5. Ozdemir V, Shear NH, Kalow W. What will be the role of pharmacogenetics in evaluating drug safety and minimising adverse effects? Drug Saf. 2001; 24:75–85. [PubMed: 11235820]
6. Pirmohamed M, Park BK. Genetic susceptibility to adverse drug reactions. Trends Pharmacol Sci. 2001; 22:298–305. [PubMed: 11395158]
7. Conrad S, Kauffmann HM, Ito K, Deeley RG, Cole SP, Schrenk D. Identification of human multidrug resistance protein 1 (MRP1) mutations and characterization of a G671V substitution. J Hum Genet. 2001; 46:656–663. [PubMed: 11721885]
8. Conrad S, Kauffmann HM, Ito K, Leslie EM, Deeley RG, Schrenk D, et al. A naturally occurring mutation in MRP1 results in a selective decrease in organic anion transport and in increased doxorubicin resistance. Pharmacogenetics. 2002; 12:321–330. [PubMed: 12042670]
9. Wang Z, Sew PH, Ambrose H, Ryan S, Chong SS, Lee EJ, et al. Nucleotide sequence analyses of the MRP1 gene in four populations suggest negative selection on its coding region. BMC Genomics. 2006; 7:111. [PubMed: 16684361]
10. Wojnowski L, Kulle B, Schirmer M, Schluter G, Schmidt A, Rosenberger A, et al. NAD(P)H oxidase and multidrug resistance protein genetic polymorphisms are associated with doxorubicin-induced cardiotoxicity. Circulation. 2005; 112:3754–3762. [PubMed: 16330681]
11. Thornalley PJ, Dodd NJ. Free radical production from normal and adriamycin-treated rat cardiac sarcosomes. Biochem Pharmacol. 1985; 34:669–674. [PubMed: 2983734]
12. Luo X, Evrovsky Y, Cole D, Trines J, Benson LN, Lehotay DC. Doxorubicin-induced acute changes in cytotoxic aldehydes, antioxidant status and cardiac function in the rat. Biochim Biophys Acta. 1997; 1360:45–52. [PubMed: 9061039]
13. Liu QY, Tan BK. Relationship between anti-oxidant activities and doxorubicin-induced lipid peroxidation in P388 tumour cells and heart and liver in mice. Clin Exp Pharmacol Physiol. 2003; 30:185–188. [PubMed: 12603349]
14. Chaiswing L, Cole MP, Ittarat W, Szweda LI, St Clair DK, Oberley TD. Manganese superoxide dismutase and inducible nitric oxide synthase modify early oxidative events in acute adriamycin-induced mitochondrial toxicity. Mol Cancer Ther. 2005; 4:1056–1064. [PubMed: 16020663]
15. Esterbauer H, Schaur RJ, Zollner H. Chemistry and biochemistry of 4-hydroxynonenal, malonaldehyde and related aldehydes. Free Radic Biol Med. 1991; 11:81–128. [PubMed: 1937131]
16. Butterfield DA, Stadtman ER. Protein oxidation processes in aging brain. Adv Cell Aging Gerontol. 1997; 2:161–197.
17. Hartley DP, Ruth JA, Petersen DR. The hepatocellular metabolism of 4-hydroxynonenal by alcohol dehydrogenase, aldehyde dehydrogenase, and glutathione S-transferase. Arch Biochem Biophys. 1995; 316:197–205. [PubMed: 7840616]
18. Volkel W, Alvarez-Sanchez R, Weick I, Mally A, Dekant W, Pahler A. Glutathione conjugates of 4-hydroxy-2(E)-nonenal as biomarkers of hepatic oxidative stress-induced lipid peroxidation in rats. Free Radic Biol Med. 2005; 38:1526–1536. [PubMed: 15890627]
19. Diah SK, Smitherman PK, Townsend AJ, Morrow CS. Detoxification of 1-chloro-2,4-dinitrobenzene in MCF7 breast cancer cells expressing glutathione S-transferase P1-1 and/or multidrug resistance protein 1. Toxicol Appl Pharmacol. 1999; 157:85–93. [PubMed: 10366541]

20. Renes J, de Vries EE, Hooiveld GJ, Krikken I, Jansen PL, Muller M. Multidrug resistance protein MRP1 protects against the toxicity of the major lipid peroxidation product 4-hydroxynonenal. Biochem J. 2000; 350(Pt 2):555–561. [PubMed: 10947971]
21. Hill BG, Awe SO, Vladykovskaya E, Ahmed Y, Liu SQ, Bhatnagar A, et al. Myocardial ischaemia inhibits mitochondrial metabolism of 4-hydroxy-trans-2-nonenal. Biochem J. 2009; 417:513–524. [PubMed: 18800966]
22. Flens MJ, Zaman GJ, van der Valk P, Izquierdo MA, Schroeijers AB, Scheffer GL, et al. Tissue distribution of the multidrug resistance protein. Am J Pathol. 1996; 148:1237–1247. [PubMed: 8644864]
23. Jungsuwadee P, Nithipongvanitch R, Chen Y, Oberley TD, Butterfield DA, St Clair DK, et al. Mrp1 localization and function in cardiac mitochondria after doxorubicin. Mol Pharmacol. 2009; 75:1117–1126. [PubMed: 19233900]
24. Jungsuwadee P, Cole MP, Sultana R, Joshi G, Tangpong J, Butterfield DA, et al. Increase in Mrp1 expression and 4-hydroxy-2-nonenal adduction in heart tissue of Adriamycin-treated C57BL/6 mice. Mol Cancer Ther. 2006; 5:2851–2860. [PubMed: 17121932]
25. Payen LF, Gao M, Westlake CJ, Cole SP, Deeley RG. Role of carboxylate residues adjacent to the conserved core Walker B motifs in the catalytic cycle of multidrug resistance protein 1 (ABCC1). J Biol Chem. 2003; 278:38537–38547. [PubMed: 12882957]
26. Senft AP, Dalton TP, Shertzer HG. Determining glutathione and glutathione disulfide using the fluorescence probe o-phthalaldehyde. Anal Biochem. 2000; 280:80–86. [PubMed: 10805524]
27. Jones DP. Radical-free biology of oxidative stress. Am J Physiol Cell Physiol. 2008; 295:C849–868. [PubMed: 18684987]
28. Zhang DW, Cole SP, Deeley RG. Identification of an amino acid residue in multidrug resistance protein 1 critical for conferring resistance to anthracyclines. J Biol Chem. 2001; 276:13231–13239. [PubMed: 11278596]
29. Ito K, Olsen SL, Qiu W, Deeley RG, Cole SP. Mutation of a single conserved tryptophan in multidrug resistance protein 1 (MRP1/ABCC1) results in loss of drug resistance and selective loss of organic anion transport. J Biol Chem. 2001; 276:15616–15624. [PubMed: 11278867]
30. Grant CE, Gao M, DeGorter MK, Cole SP, Deeley RG. Structural determinants of substrate specificity differences between human multidrug resistance protein (MRP) 1 (ABCC1) and MRP3 (ABCC3). Drug metab dispos. 2008; 36:2571–2581. [PubMed: 18775981]
31. Hubatsch I, Ridderstrom M, Mannervik B. Human glutathione transferase A4-4: an alpha class enzyme with high catalytic efficiency in the conjugation of 4-hydroxynonenal and other genotoxic products of lipid peroxidation. Biochem J. 1998; 330(Pt 1):175–179. [PubMed: 9461507]
32. Ishikawa T, Esterbauer H, Sies H. Role of cardiac glutathione transferase and of the glutathione S-conjugate export system in biotransformation of 4-hydroxynonenal in the heart. J Biol Chem. 1986; 261:1576–1581. [PubMed: 3753704]
33. Deeley RG, Westlake C, Cole SP. Transmembrane transport of endo- and xenobiotics by mammalian ATP-binding cassette multidrug resistance proteins. Physiol Rev. 2006; 86:849–899. [PubMed: 16816140]
34. Jungsuwadee, P.; Vore, M. Efflux Transporters in Comprehensive Toxicology, Editor-in-Chief, Charlene A. McQueen. In: Guengerich, FP., editor. Biotransformation. 2ed. Elsevier; 2010. p. 557-601.Chapter 26
35. Stride BD, Cole SP, Deeley RG. Localization of a substrate specificity domain in the multidrug resistance protein. J Biol Chem. 1999; 274:22877–22883. [PubMed: 10428874]

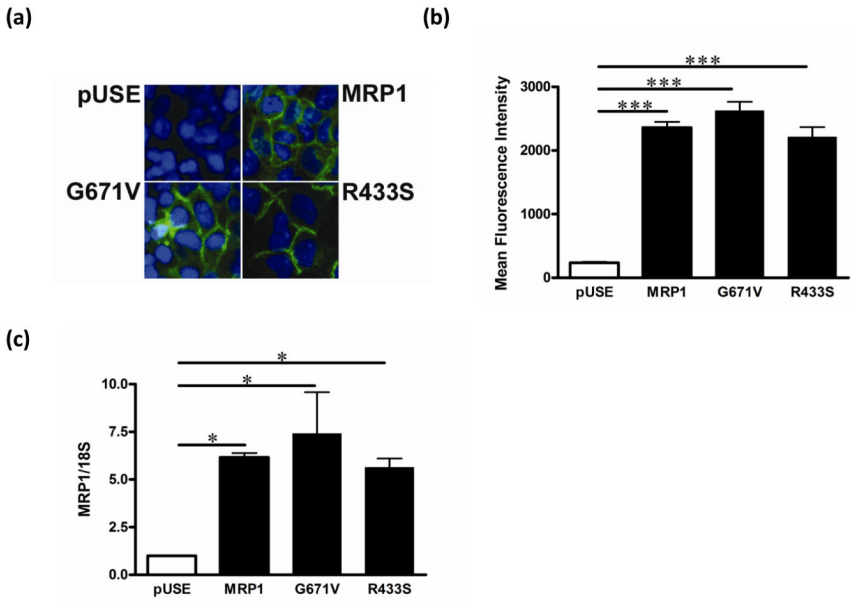

Fig. 1. Expression in stable cell lines of multidrug resistance-associated protein 1 (MRP1) and is variants

(a) Cells were immunostained for MRP1 protein; blue = nuclei, green = MRP1 protein. Plasmids containing wild-type MRP1 or the MRP1 variants G761V and R433S were transfected into HEK293 cells to generate stable cell lines. pUSE cells were HEK293 cells transfected with pUSEamp(+) empty vector and used as a control. (b) Cells were stained with MRPr1 primary antibody, followed by fluorescence labeled secondary antibody (AlexaFlor488) for flow cytometry analyses. Bar graphs show mean fluorescence intensity ± S.E. (c) MRP1 mRNA expression was detected by real time RT-PCR and normalized by 18S rRNA expression. * $P < 0.05$, *** $P < 0.001$.

(a)

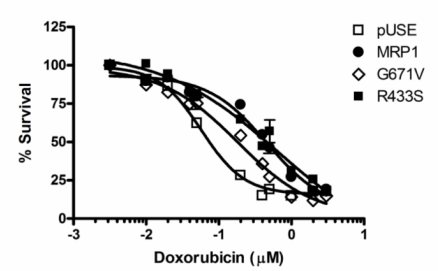

(b)

Genotype	Doxorubicin IC_{50} nM (95% CI)
pUSE	58.0 (51.4-65.5)
MRP1	463.0 (332.7-644.2)
G671V	181.4 (137.4-239.5)
R433S	645.2 (158.3-2630.0)

Fig. 2. Percent survival of HEK_{pUSE}, HEK_{MRP1}, HEK_{R433S}, and HEK_{G671V} cells in the presence of DOX

(a) Cells were seeded into 96-well plates and cultured in the presence of DOX for 48 h. After 48 h of cell culture, the MTT assay was performed as described in Methods. (b) The concentrations of DOX that inhibited cell survival by 50% were calculated using non-linear regression.

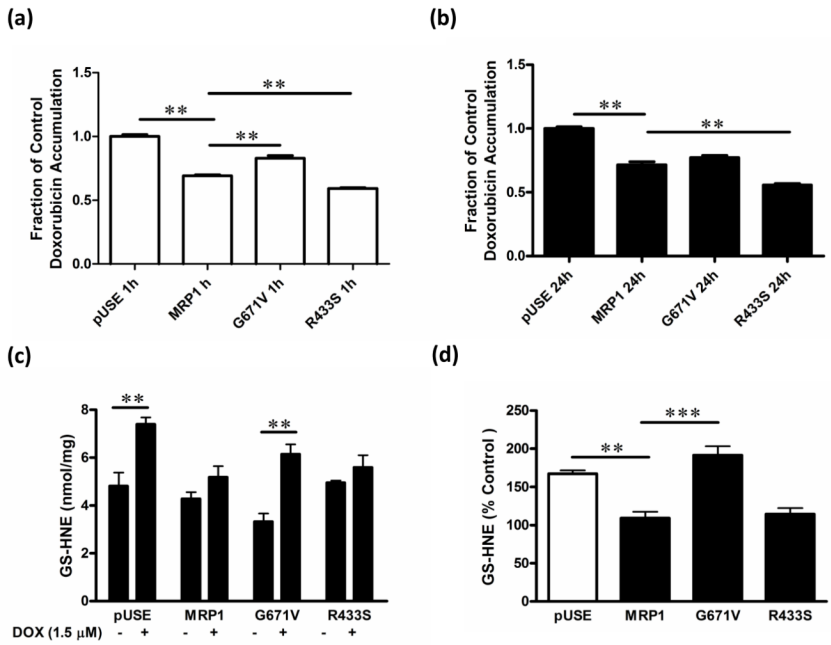

Fig. 3. DOX and GS-HNE retention in HEK_{pUSE}, HEK_{MRP1}, HEK_{R433S}, and HEK_{G671V} cells

(a) Cells were cultured in the presence or absence of 50 μM DOX for 1 h, followed by a 30 min efflux period, and analyzed for intracellular DOX by fluorescence spectrophotometry. (b) Cells were cultured in media alone or in the presence of DOX (1.5 μM) for 24 h. Cells were harvested, lysed and intracellular concentrations of DOX (c) and GS-HNE (d) determined. (d) The concentration of GS-HNE in cells expressed as a percentage of that in HEK_{MRP1} cells. ** $P < 0.01$, *** $P < 0.001$

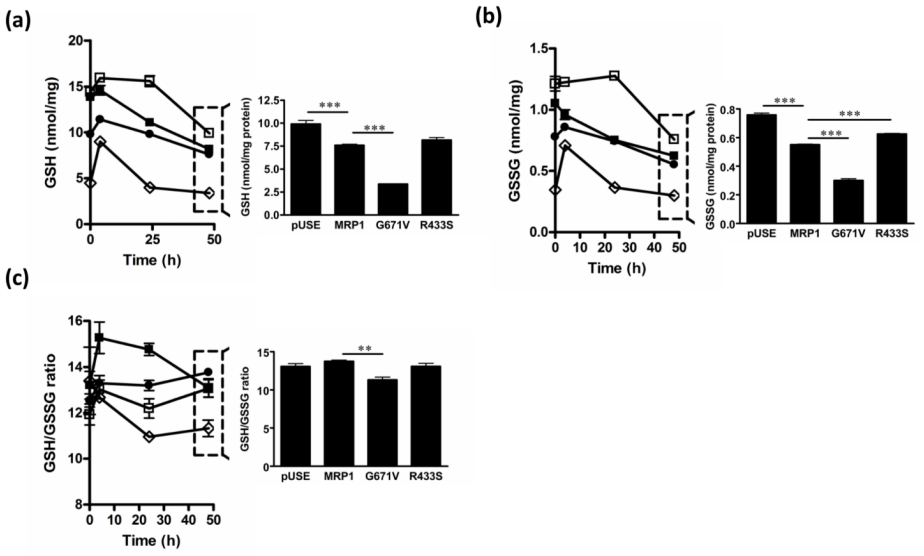

Fig. 4. Time-course of intracellular GSH and GSSG in HEK_{pUSE}, HEK_{MRP1}, HEK_{R433S}, and HEK_{G671V} cells

Cells were cultured in media alone or in the presence of DOX (0.5 μM) for 4, 24 and 48 h. Cells were harvested, lysed and intracellular concentrations of (a) GSH, (b) GSSG determined and (c) the GSH/GSSG ratio calculated. The embedded bar graphs represent the data obtained from cells treated with DOX for 48 h. ** $P < 0.01$ and *** $P < 0.001$. HEK_{pUSE}, open square; HEK_{MRP1}, closed circle; HEK_{R433S}, closed square; and HEK_{G671V}, open diamond.

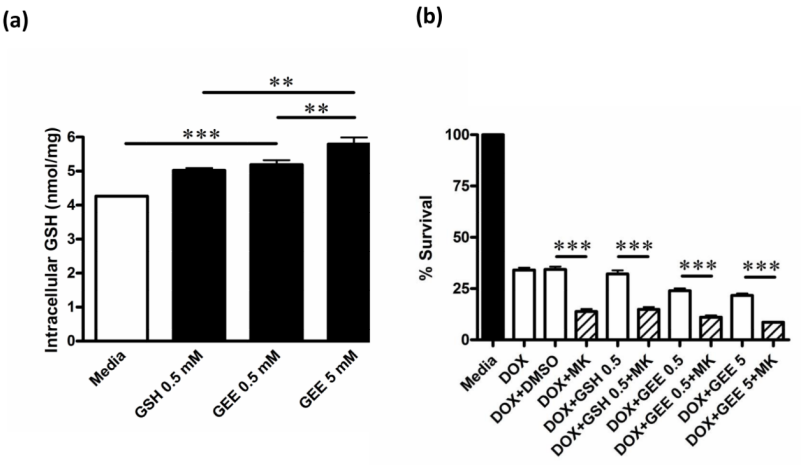

Fig. 5. Supplementation of DOX-treated HEK$_{G671V}$ cells with GSH or GEE

(a) HEK$_{G671V}$ cells were cultured in media alone or in the presence of GSH (0.5 mM) or GEE (0.5 and 5 mM) for 48 h. Cells were harvested, lysed and intracellular concentrations of GSH determined by HPLC. (b) HEK$_{G671V}$ cells were cultured in the presence of 0.5 μM DOX and in media supplemented with GSH (0.5 mM) or GEE (0.5 and 5 mM) in the presence or absence of MK571 (MK; 20 μM) for 48 h, and the percent of viable cells determined by the MTT assay. ** $P < 0.01$ and *** $P < 0.001$.

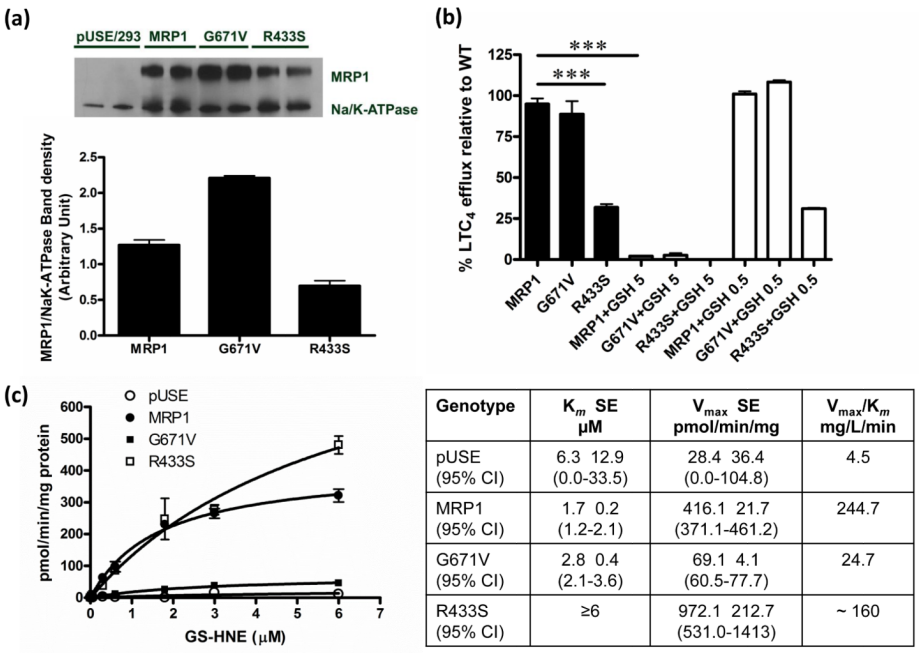

Genotype	K_m SE μM	V_{max} SE pmol/min/mg	V_{max}/K_m mg/L/min
pUSE (95% CI)	6.3 12.9 (0.0-33.5)	28.4 36.4 (0.0-104.8)	4.5
MRP1 (95% CI)	1.7 0.2 (1.2-2.1)	416.1 21.7 (371.1-461.2)	244.7
G671V (95% CI)	2.8 0.4 (2.1-3.6)	69.1 4.1 (60.5-77.7)	24.7
R433S (95% CI)	≥6	972.1 212.7 (531.0-1413)	~ 160

Fig. 6. [^{3}H]LTC$_4$ transport activities of HEK$_{MRP1}$, HEK$_{R433S}$, and HEK$_{G671V}$

(a) Western analysis of MRP1 and Na/K-ATPase$_{\alpha 1}$ protein expression in plasma membranes from HEK$_{pUSE}$, HEK$_{MRP1}$, HEK$_{R433S}$, and HEK$_{G671V}$ cells. (b) ATP-dependent transport of 100 nM [^{3}H]LTC$_4$ in plasma membrane vesicles from HEK$_{MRP1}$, HEK$_{R433S}$, and HEK$_{G671V}$ cells in the absence (closed bars) or presence (open bars) of 5 or 0.5 mM GSH. (c) ATP-dependent transport of [^{3}H]GS-HNE (0 – 6 μM) in plasma membrane vesicles from HEK$_{MRP1}$, HEK$_{R433S}$, HEK$_{G671V}$ and HEK$_{pUSE}$ cells. Kinetic parameters for ATP-dependent [^{3}H]GS-HNE transport calculated from transport studies. Data represent mean ± SE from triplicate determinations (n = 3 per group). *** $P < 0.001$. All data were normalized for expression of MRP1.

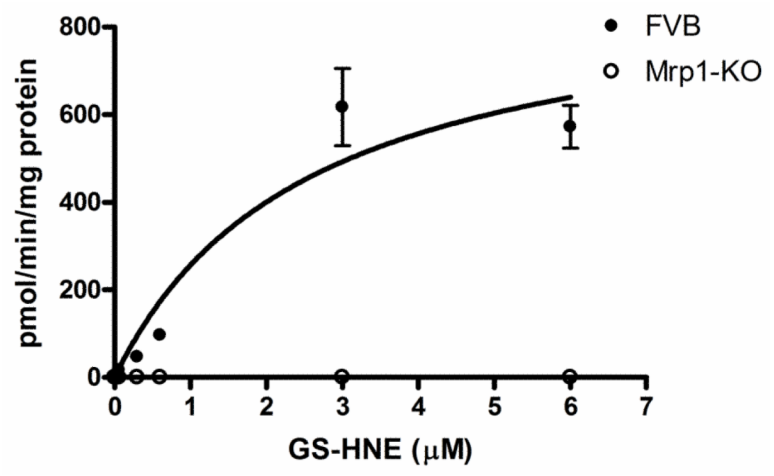

Fig. 7. ATP-dependent transport of GS-HNE by Mrp1

ATP-dependent transport of [^{3}H]GS-HNE determined in sarcolemma membrane vesicles obtained from FVB and Mrp1$^{-/-}$ mice treated with DOX (20 mg/kg, i.p.) and killed 24 h later. Data represent the mean ± SD from triplicate determinations (n = 3 per group).